Thermodynamic Optimization Tools for Power Tracking in a Multistage Concentrated Solar Power Rankine Plant

P. N. Nwosu[1]; A. Nurick[2]; and E. T. Akinlabi[3]

Abstract: The object of the study is to present a method of thermodynamic optimization of power generating plants, in a mode that consolidates and simplifies the analysis of data on heat-work interaction of the plant components. The optimization scheme identifies the technical and process parameters that can improve the thermodynamic performance of the plant with respect to an objective variable, and further, the required thermodynamic measures necessary to improve the operating condition of the plant. Simple but effective tools are used to evaluate the optimal and suboptimal power generating capacities vis-à-vis the fundamental variables—namely, the thermodynamic quantity ratio (TQR) and the power-energy quantity ratio (PQR)—without routing optimization procedures. Beyond the optimal value of the objective variable, the power generation capacity of the plant is affected. The determination of the optimal value of the objective variable can also be approached by computerization; for fixed prescriptions of the boiler, superheater, and turbine parameters, variables such as boiler pressure and temperature can be optimally selected. DOI: 10.1061/(ASCE)EY.1943-7897.0000367. © 2016 American Society of Civil Engineers.

Author keywords: Thermal efficiency; Thermodynamics analysis; Energy recovery; Optimization; Temperature; Pressure.

Introduction

The object of the study is to present a method of thermodynamic optimization of power generating plants, in a mode that consolidates and simplifies the analysis of data on heat-work interaction of the plant components.

A concentrated solar power (CSP) plant operating on the basis of Rankine cycle is considered. Relatively, solar energy is plentiful in certain parts of the world for large-scale thermal-electricity generation of which the major benefit of the resource is that it is free, renewable, and friendly to the environment. This has prompted current attention toward alternative fuel sour-ces. The CSP technology is promising for large-scale power generation. With relatively abundant solar radiation potentials in Sub-Saharan Africa, there are currently few CSP operational plants.

Monitoring temperature and pressure continually in a thermal plant among other process variables entails data profiling, which is fundamental to analyzing and improving the heat-work relation in a thermodynamic process. The process of power generation in a power plant is mostly driven by temperature-pressure dynamics, among other process variables. The pressure and temperature required to raise the working fluid to a reasonable degree of super-heat are a substantial part of the operating expense of the plant. This also determines the selection and design of the functional components of the plant, as well as the system efficiency and operating cost. The optimization of these fundamental thermodynamic variables therefore is critical to maintaining profitable, efficient operations especially in environments where sustainability is a primary concern.

Research into power plant operations and optimization has elicited some interest (Mu et al. 2015; Li et al. 2013). A number of optimization studies have led to different methodology, most of which are based on standard optimization relations (Clarke 2014), and the entropy generation method (EGM) (Yekoladio et al. 2015). Badr et al. (1985) simulated the performance of Rankine-cycle power-plants, which used steam as the working fluid, and developed a BASIC program to facilitate the prediction of the optimal design conditions. Kapooria et al. (2008) conducted a theoretical investigation into a Rankine cycle plant and observed that the efficiency can be improved by using an in-termediate reheat cycle. A study conducted by Ho et al. (2012) compared the organic flash cycle (OFC) to other advanced vapor cycles for intermediate and high temperature waste heat reclama-tion and solar thermal energy applications, and concluded that aromatic hydrocarbons are better suited to the organic Rankine cycle (ORC) and OFC working fluids; due to their higher power output; also the fluids require less complex turbine designs. Although the OFC improved heat addition and the exergetic efficiency, this advantage was negated by irreversibilities intro-duced during flash evaporation. Huijuan et al. (2010) reviewed and discussed the organic Rankine cycle and supercritical Rankine cycle for the conversion of low-grade heat into electrical power, as well as the selection criteria for potential working flu-ids; screening 35 working fluids for the two cycles and analyzing the influence of the fluid properties on the cycle performance. They concluded that the thermodynamic, and physical properties, stability, environmental impacts, safety and compatibility, and availability and cost are important considerations for selecting a working fluid. Ankur and Khandwawala (2013) obtained cor-rection curves for power output by reason of the conflicts between the actual and predicted output values of a 120 MW thermal

[1]Postdoctoral Associate, Dept. of Mechanical Engineering Science, Univ. of Johannesburg, Auckland Park 2006, South Africa (corresponding author). E-mail: paul.nwach@gmail.com

[2]Professor, Dept. of Mechanical Engineering Science, Univ. of Johannesburg, Auckland Park 2006, South Africa. E-mail: alann@uj.ac.za

[3]Professor, Dept. of Mechanical Engineering Science, Univ. of Johannesburg, Auckland Park 2006, South Africa. E-mail: etakinlabi@uj.ac.za

power plant, with combined effect of constant inlet pressure (124.61 bar) and different inlet temperatures. Nouman (2012) conducted comparative studies and analyses of working fluids for organic Rankine cycles. It was determined that the tempera-ture profile in the evaporator and condenser influenced exergy losses and the best energy utilization potential. It was noted that sometimes the condenser and evaporator pressure limited the use of some working fluids. Studies on optimization techniques into various thermal plant processes include those of Wanga et al. (2013), in which a study was undertaken to analyze and optimize an ORC using a low-grade heat source; a ratio of net power output to total heat transfer area was obtained and used as the performance evaluation criterion. Roy and Misra (2012) conducted a parametric optimization and performance analysis of a regenerative organic Rankine cycle using R-123 for waste heat recovery; consequently developed a computer program to parametrically optimize and compare the system using the second law efficiency; turbine work output; system mass flow rate; and irreversibility rate.

The benefits of evaluating the fundamental variables sway energy expense and work output, which are significant factors in maintaining efficiency and profitability. It becomes important therefore to develop simple but effective tools that render operational data in an easy-to-read form for visual analysis and optimization. In this study, the thermodynamic quantity ratio (TQR) and power-to-energy quantity ratio (PQR) are defined for the optimization scheme, such that any change in one or more process variables can be easily inferred graphically, or by computerization. Using the TQR, the authors show that classical efficiency index does not indicate the point of optimal operations, hence it is inadequate. In addition, the methodology employed here can be applied to other Rankine cycle plant designs.

Cycle Description

The CSP thermal plant is purpose-built for continuous operation during both sunny and dark periods; this is facilitated by a thermocline or heat (salt) storage vessel which increases the number of full load operations during nocturnal operating periods. The equivalent thermodynamic cycle of the Siemens CSP thermal plant (Siemens AG 2010) is given in Fig. 1. The working fluid is heated by a solar field (CSP panels), and the heat is transferred to the steam heat exchangers to boil vaporize, superheat and reheat the working fluid. The cycle starts with the saturated feedwater (working fluid) leaving pump 2 to the boiler where it is preheated, bypassing onto the salt storage tank for other thermal applications, then is delivered to the superheater where it is superheated to high temperature and pressure. The exiting fluid is then delivered to the high pressure (HP) turbine to generate power; subsequently is reheated to gain heat at low pressure and fed to the low pressure (LP) turbine to generate additional power. The exiting low-pressure fluid expands in the condenser and regenerators, i.e., the open feed water heater (OFWH) or deaerator and the closed feed water heater (CFWH), where it loses heat to a heat sink. The pumping power for the latter operation is delivered by Pump 1. Fig. 2 shows the temperature entropy ($T - s$) diagram and the nodal representations of the thermodynamic cycle.

Thermodynamic Analysis

Typically, the Rankine cycle is analyzed as a steady-state flow process (Yunus and Michael 2006). The changes in kinetic and potential energy are negligible in the steam relative to the work and heat transfer quantities. The steady-state flow mass and energy equations per unit mass of steam can be written as

$$\dot{Q} - \dot{W} = \sum_{out} \dot{m}(h) - \sum_{in} \dot{m}(h) \qquad (1)$$

The energy balance is based on the first principles. The general exergy balance for a steady flow system is given by Yunus and Michael (2006)

$$\dot{Q} - \dot{W} = T_o \sum_{out} \dot{m} s_{\_} - \sum_{out} \dot{m} s_{\_} \qquad (2)$$

In terms of irreversibility, the exergy losses are indicative of energy and work potential losses in a thermodynamic system, and the system irreversibility.

On per unit mass basis for a single inlet, exit, steady flow process (Yunus and Michael 2006), then

$$\chi_{dest} = T^o S_{gen} = T^o \left(S_e - S_i \right) \frac{\dot{q}_{out}}{\_} \; : \; \frac{\dot{q}_{in}}{\_} \qquad (3)$$

where S_{gen} = generated entropy; s = entropy; $T_{b;in}$ and $T_{b;out}$ = temperatures of the system boundaries in which heat is transferred. The exergy destruction for a cycle with high-temperature and low-temperature reservoirs on per unit mass basis is expressed as (Yunus and Michael 2006)

$$\chi_{dest} = T^o S_{gen} = T^o \sum_{out} \frac{\dot{q}_{out}}{x} - \sum_{out} \frac{\dot{q}_{in}}{x} \qquad (4)$$

Considering the source and sink temperatures in the cycle, the equation reduces to (Yunus and Michael 2006)

$$\chi_{dest} = T^o S_{gen} = T^o \left(\frac{\dot{q}_{out}}{T_L} - \frac{\dot{q}_{in}}{T_H} \right) \qquad (5)$$

where T_H and T_L are the source and sink temperatures, respectively. For a fluid stream ψ, the exergy at any state of the fluid can be determined from (Yunus and Michael 2006)

$$\psi = (h - h_0) - T^o (h - h_0) + \frac{v^2}{2} + gz \qquad (6)$$

in which h = enthalpy; v = velocity; and T = temperature; 0 denotes the state boundaries. The thermal efficiency gives an indication of the energy conversion potentials. The thermal efficiency is given by

$$\eta_{th} = \frac{\dot{W}_{net}}{\dot{Q}_{in}} = \frac{\dot{Q}_{in} - \dot{Q}_{out}}{\dot{Q}_{in}} \qquad (7)$$

Importantly, the previous equations are applied at the cycle nodes, which reference the thermodynamic state functions while maintaining conservation laws. Assuming adiabatic conditions for the turbines, consequently

$$E_{in} - E_{out} \rightarrow \sum_{in} \dot{m} h = \sum_{out} \dot{m} h \qquad (8)$$

Therefore, mass and energy conservation is maintained.

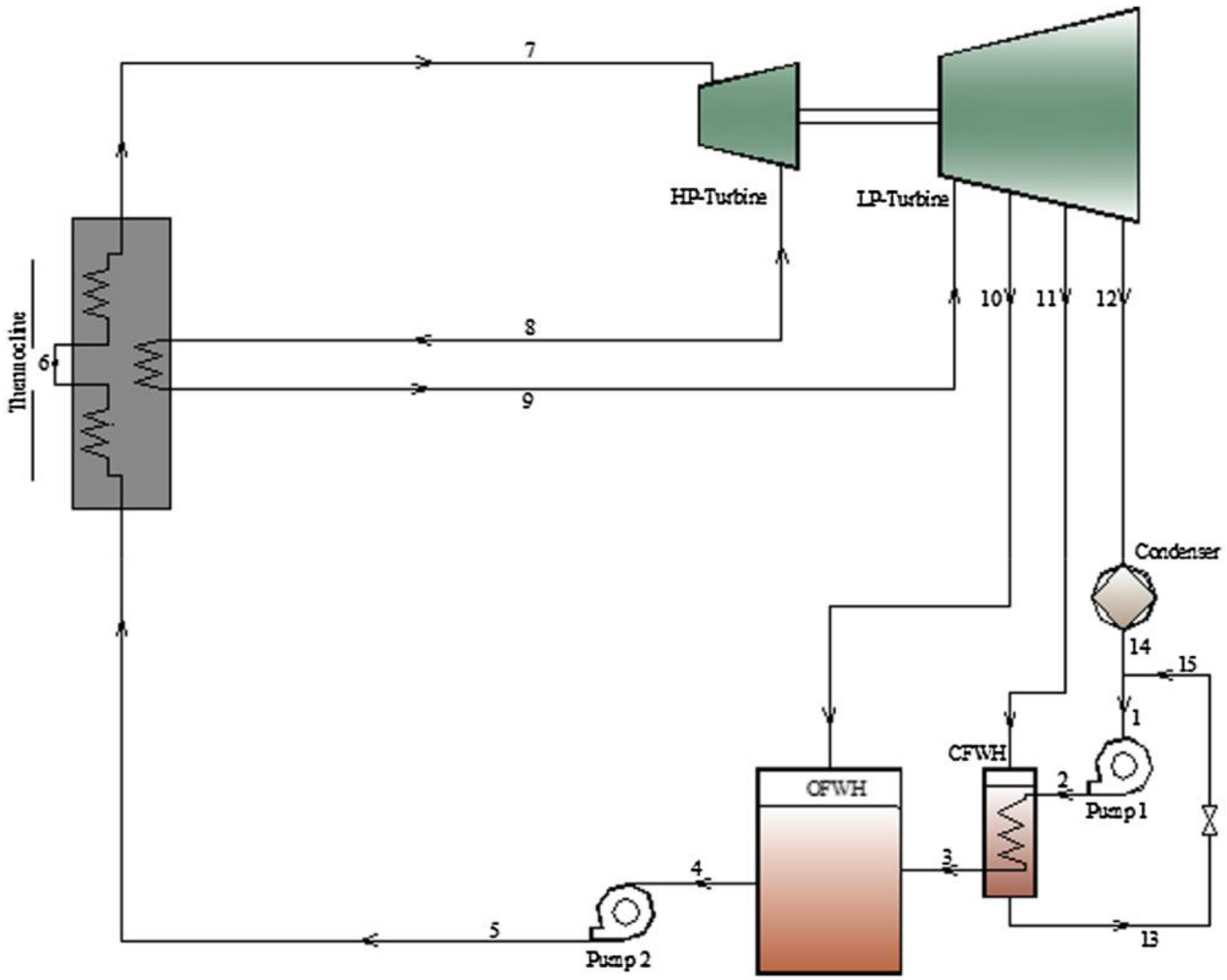

Fig. 1. Schematic diagram of the CSP plant

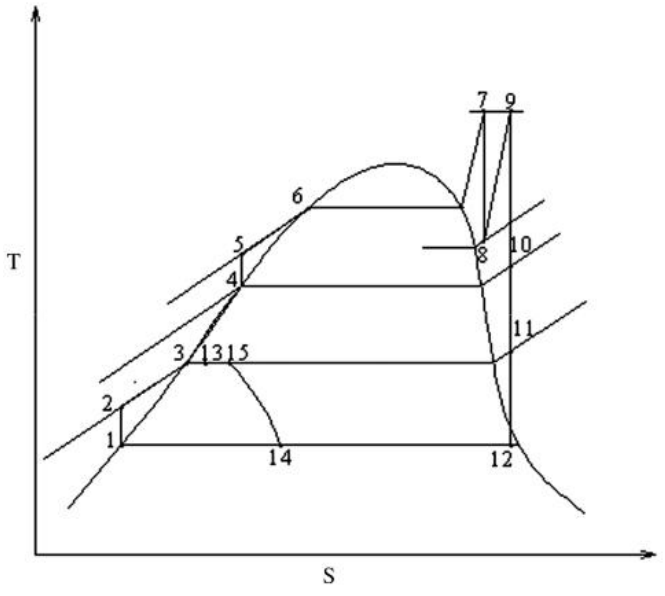

Fig. 2. Temperature-entropy (T − s) diagram of the Rankine cycle

Modeling Assumptions

The following theoretical assumptions are the underlying stand-points of the modeling scheme:

- The power plant operates in an ideal isentropic process, as such there is negligible pressure drop in the boiler, superheater and condenser. Steam exits the condenser and regenerator as saturated fluid;
- The temperature and pressure of the boiler (main flow preheater) and evaporator (superheater) are based on a range of operating temperatures and pressures of operating, commercial power plants;
- The pump operates with negligible losses and the efficiency is assumed to be 100%;
- The effectiveness of the heat exchange process in the boiler and superheater, and recuperator are assumed to be ideal;
- Pressures are constant in the condenser and pumps, with negligible losses;
- The turbine is adiabatic and the working fluid expands isentropically;
- The losses in the flow pipes are negligible;
- A further assumption is that recuperator is hermitically sealed; and

- Steam is used as the working fluid as an alternative to organic working fluids.

Theory and Models

The energy relations are calculated on the basis of the enthalpy functions, determined by the state properties obtained at each nodal point. The engineering equation solver (EES) program was used in the computation of the thermodynamic functions by reason of its unique functionality. In Fig. 1, the HP turbine expands the steam adiabatically; the steam is reheated and delivered to the LP turbine, where it also expands adiabatically. The LP turbine generates additional power from the reheated fluid by driving a generator attached to it. The degree of superheat depends on the operational thermodynamic parameters. The energy fraction of the steam extracted by the turbines can be determined from the following energy and mass balances:

$$\dot{Q} \cong \dot{W} \cong \dot{k}e \cong \dot{p}e \qquad (9)$$

$$\dot{E}_{in} - \dot{E}_{out} = \dot{E}_{system} \qquad (10)$$

$$\Rightarrow \sum \dot{m}_i h_i = \sum \dot{m}_e h_e \qquad (11)$$

Considering the form of the equation, the summation of the work done by the HP and LP turbines can be written as

$$\dot{W}_t = \sum \dot{m}_i h_i \qquad (12)$$

$$\dot{W}_t = (h_7 - h_8) + (h_9 - h_{10}) + (1 - m_1)(h_{10} - h_{11}) + (1 - m_1 - m_2)(h_{11} - h_{12}) \qquad (13)$$

Conservation of energy and mass is maintained. For convenience, we assume the points between the OFWH and CFHW, and the condenser and Pump 1 are in thermal equilibrium, such that the energy balance for the OFWH (deaerator) is

$$(1 - m_1)h_3 + m_1 h_{10} = h_4 \qquad (14)$$

and

$$m_2 h_{11} + (1 - m_1)h_2 = (1 - m_2)h_3 \qquad (15)$$

The energy balance for the nodal junction between the condenser and the Pump 1 is given by

$$(1 - m_1 - m_2)h_{14} + m_2 h_{13} = (1 - m_1)h_1 \qquad (16)$$

The mass fractions m_1 and m_2 can be evaluated by solving the foregoing equations. Work done by Pumps 1 and 2, respectively, are given by

$$\dot{W}_{p1} = (1 - m_1)(h_1 - h_{12}) = (1 - m_1) \cdot v(P_1 - P_{12}) \qquad (17)$$

and

$$\dot{W}_{p2} = (h_5 - h_4) = v(P_5 - P_4) \qquad (18)$$

The heat input and output are determined from the enthalpy functions can be obtained by considering the heat balance in the boiler/vaporizer, superheater and the reheater, such that

$$\dot{Q}_{boil:} = (h_6 - h_5) \qquad (19)$$

$$\dot{Q}_{sup} = (h_7 - h_6) \qquad (20)$$

$$\dot{Q}_{reh:} = (h_9 - h_8) \qquad (21)$$

And the heat output of the condenser is given by

$$\dot{Q}_{cond:} = (1 - m_1 - m_2) \cdot (h_{12} - h_{14}) \qquad (22)$$

where $\dot{Q}_{boil:}$, $\dot{Q}_{sup}$, $\dot{Q}_{reh:}$ and $\dot{Q}_{cond.}$. are the heat input/output in the boiler, superheater, reheater, and the condenser, respectively. The thermal efficiency, which gives an indication of the system potential for converting heat to useful work, can be determined from the gross heat input and net work output, hence

$$\eta_{th} = \frac{\dot{W}_{net}}{\dot{Q}} = \frac{\dot{W} - (\dot{W}_t + \dot{W}_{p1} + \dot{W}_{p2})}{\dot{Q}_{boil:} + \dot{Q}_{vap:} + \dot{Q}_{reh:}} \qquad (23)$$

The capacity of the plant to generate power is determined from

$$\dot{P}_{gen} = \dot{m}_t[(h_7 - h_8) + (h_9 - h_{10}) + (1 - m_1)(h_{10} - h_{11}) + (1 - m_1 - m_2)(h_{11} - h_{12})] \qquad (24)$$

where m_1, m_2, and $(1 - m_1 - m_2)$ are the steam fractions and $\dot{m}_t$ is the flow rate of the working fluid.

Thermodynamic Quantity Ratio

An embodiment of the present methodology involves modeling the process (thermodynamic) quantities, which gives an indication of the operational performance with respect to the optimization ob-jectives. The benefit is that with simplified, concise models the relevant quantities can be rendered in graphical plots in an impactful perspective, which could save operational costs, and decision times. A further embodiment is a methodology enabling operational data to be profiled in attaining an optimal power production state.

There are distinctly two main approaches to thermodynamic optimization of the process parameters in a power plant (Clarke 2014; Yekoladio et al. 2015): one in which the problem is formulated as a standard optimization problem with the aim of choosing a set of decision variables that maximize the objective function (Clarke 2014), and the other based on entropy EGM (Yekoladio et al. 2015), which leads to the choice of an objective variable. Both tech-niques present unique ways of optimizing the objective function, but could lead to complex routines due to their procedures.

Defining the following variables:

$$\dot{Q}_{s;cyc} = \sum \dot{P}_{Hi} \qquad (25)$$

$$\dot{W}_{s;cyc} = \sum \dot{P}_{Hi} \qquad (26)$$

$$= \dot{W} \qquad (27)$$

where

$$X_{Hi} = X_{Qi} + X_{Wi} \qquad (27)$$

For specific plant components, the heat input quantity is given by

$$Q_s \quad \frac{Q}{P_{i;s}} \qquad 28$$

$$= P \qquad (P$$

$$TQR_{cyc} = Q_{s;cyc} + W_{s;cyc} \qquad (29)$$

and

$$TQR = Q_s + W_{s;cyc} \qquad (30)$$

where $Q_{i;s}$ = summation of the heat input into the plant (excluding heat output or rejection in the condenser); Q_i = summation of the heat input and output in the plant; W = summation of the work input and output in the plant. $W_{s;cyc}$ = proportion of total (cycle) work input and output in the plant; $Q_{s;cyc}$ = proportion of total (cycle) heat input and output in the plant; and Q_s = proportion of heat input into the plant.

PQR Criterion

Comparatively, the thermodynamic and economic optimization measures are approached by considering the objectives of operating the plant with the maximum thermodynamic and techno-economic benefits. By determining the input and output variables required to operate the plant in a thermodynamically optimal state vis-à-vis cost-effective operations, the maximum potential of the thermody-namic and cost-effective objectives can be realized. Defining the power-energy quantity ratio (PQR)

$$PQR = \frac{Pgen \cdot W_s}{Q_s} \qquad (31)$$

enables the optimal fuel-to-power expense be determined.

The determination of the potential power generation returns with respect to the optimal operating state of the plant, i.e., the income generated by the plant in converting a KJ of fuel to power in a day in suboptimal operating conditions is of important benefit to cost-effective operations. Defining the power generation returns (PGR) on investment as

$$PGR = \hbar \cdot Q_s \quad i \quad Q_{s;opt} \qquad (32)$$
$$\frac{Pgen}{} \quad \frac{Pgen_{opt}}{}$$

where $\hbar$ is the returns or income of operating the plant on optimal conditions on daily basis in $ per KW power per KW fuel (i.e. the income generated by the plant by converting a KJ of fuel to KW power in a day). The margin and deviation from the thermodynami-cally and economically optimal operating state of the plant can be determined from the above relation.

In addition, identifying the economic loss potential in comparing the actual operating condition with the optimal operating condition will lead to operational modifications taking into account improved energy efficiency. Defining the daily suboptimal income (SIC) relation as

$$SIC\ losses = \hbar \cdot 1 - Q_{s;i\ i} \quad Q_{s;opt} \qquad (33)$$
$$\frac{Pgen}{} \quad \frac{Pgen_{opt}}{}$$

consequently, on an annual basis; the above becomes

$$Annual\ SIC\ losses = 365\ days \cdot SIC\ losses \qquad (34)$$

Similarly, the determination of the relative margin and loss pro-file due to suboptimal power generating condition with respect to an objective variable, enabling rapid assessment and real-time de-cisions is beneficial in the assessment of operational losses given by the suboptimal power generation (SPG) losses

$$SPG\ losses = 1 - Q_s \quad i \quad Q_{s;opt} \qquad (35)$$
$$\frac{Pgen}{} \quad \frac{Pgen_{opt}}{}$$

Accordingly, these relations are useful in determining the margin of suboptimal operations, as it relates to the optimal operating condition of the plant, and the margin of potentially accruable returns in order to identify technical enhancement measures which are needed for optimal performance.

Results and Discussion

TQR Chart

The case study is focused on a concentrated solar power plant, operating on multistage turbines. The plant is based on an advanced CSP design and requires the model equations be evaluated over the complex plant system. Data typical of a running plant are used to evaluate the models. The process parameters are itemized in Tables 1–4 for P_{vap} and T_{vap}.

Importantly, the manner in which operational data and results of any optimization scheme are rendered can influence decision times, and workflow. The plot of the cycle heat and workflow quantities by means of the (cycle) thermodynamic quantity ratio (TQR_{cyc}) and thermodynamic quantity ratio (TQR) indicating the profile, and the overall change in the heat-work interaction of various plant components with respect to a decision variable is presented. The difference between TQR_{cyc} and TQR is that the former is useful in plotting the variation of the heat and work quantities of the plant, while the latter can be applied in generating interconnected plots for graphic-based optimization and computerization.

Obtained on the basis of the TQR_{cyc} relation, the pie charts in Fig. 3 shows the relative proportions of the individual rate equations; $Q_{boil.}$, $Q_{reh.}$ $Q_{sup;}$, $Q_{cond.}$, W_{turb}, W_{p1} , and W_{p2} are defined relative to the overall (cycle) thermodynamic variables. Supposing the pressure of the superheater (which is the pump pressure) was varied from 5 to 20 MPa, one could evaluate the relative change in the quantities previously mentioned. If one were to plot a different set of curves for this operational scenario using typical efficiency plots, it would result in ambiguities, however, the TQR_{cyc} plot (Fig. 4) at a glance depicts the operational dynamics of the plant with respect to the (objective) variables. $Q_{s;cyc}$ and $W_{s;cyc}$ include all the cycle heat and work quantities, respectively. At P_{vap} = 5 MPa, the proportion of heat supplied to the boiler (37.40%) is

Table 1. Process Parametric Values of TQR_{cyc} for Fig. 3

Pressure	Value (KPa)	Temperature	Value (°C)
P_{12}	10	T_3	150
P_2	1,200	T_9	400
P_8	800	—	—
P_{10}	100	—	—
P_{14}	1,000	—	—
P_{11}	800	—	—

Table 2. Itemization of Results for Calculation of TQR_{cyc} for Fig. 3

P_5 (kPa)	$W_{s;cyc}$ (%)	$Q_{s;cyc}$ (%)	η_{th}	P_{gen} (MW)	PQR
5	16.9	46.24	0.3621	10.11	3.695047578
10	17.74	45.05	0.3868	11.301	4.45016071
20	17.78	42.88	0.3992	10.61	4.399388993

Table 3. Process Parametric Values of TQR_{cyc} for Fig. 4

Pressure	Value (kPa)	Temperature	Value (°C)
P_{12}	10	T_3	150
P_2	1,200	T_9	400
P_8	800	—	—
P_{10}	100	—	—
P_{14}	1,000	—	—
P_{11}	800	—	—

Table 4. Itemization of Results for Calculation of TQR_{cyc} for Fig. 4

T_5 (°C)	$W_{s;cyc}$ (%)	$Q_{s;cyc}$ (%)	η_{th}	P_{gen} (MW)	PQR
400	14.41	20.44	12.37	17.5458	0.4105
500	17.83	21.70	14.52	17.67156	0.4359
600	20.71	22.93	16.84	18.641	0.4604

high with relatively low turbine work (18.87%), compared to 34.94% and 20.44% at P_{vap} = 10 MPa, hence the need for a visual approach, and the optimization methodology, which at a glance shows the heat and mass quantities with respect to an objective variable. This differs from the other procedures.

Likewise, for varying vaporizer temperature, the pie charts in Figs. 4(a and b), show plots of the TQR_{cyc} quantities, and the relative proportions of the individual rate equations, defined on the basis of the overall (cycle) thermodynamic variables.

Otherwise, the graphical optimization routine, which entails plotting the interconnected graphs of the thermodynamic quantities and selecting the value of the objective variable, can also be approached by computerization, defining TQR^nðix; jyÞ; σ½TQR^nðix; jyÞ&, where σ is a set, and subscripts x and y are the orders of magni-tudes of the variables in the maximum-to-minimum sequence; i; j are the considered quantities; in this case overall work (i) and overall heat input ðjÞ; n is the number of such combi-nation, one could write σ_{max}½TQR^1ðix; j yÞ; TQR^2ði; jÞ : : : & and σ_{min}½TQR^1ðimax; jmin Þ; TQR^1 ðimin; jmax Þ; : : : &. The set of thermo-dynamic quantities which conform to the (optimal) design/ operational criterion given by the set can be obtained. The process can be efficiently computerized for real-time analysis without re-course to complex optimization techniques.

Thermal Efficiency versus PQR

An examination of the power plant operations given the fundamen-tal thermodynamic variables is of important benefit in streamlining operations, as well as in effecting necessary control measures re-quired to optimize performance. The influence of the vaporizer pressure on the process parameters is shown in Fig. 5, which underscores the fact that the point at which the plant operates with maximum thermal efficiency does not necessarily entail the point of optimal operation, in terms of fuel-to-power conversion potential. In Fig. 5, at the point of maximum thermal efficiency, the heat addition into the plant (Q_s) is relatively high per KW power gen-erated compared to that at the cusp of Q_s and minimum $W_{s;cyc}$ with

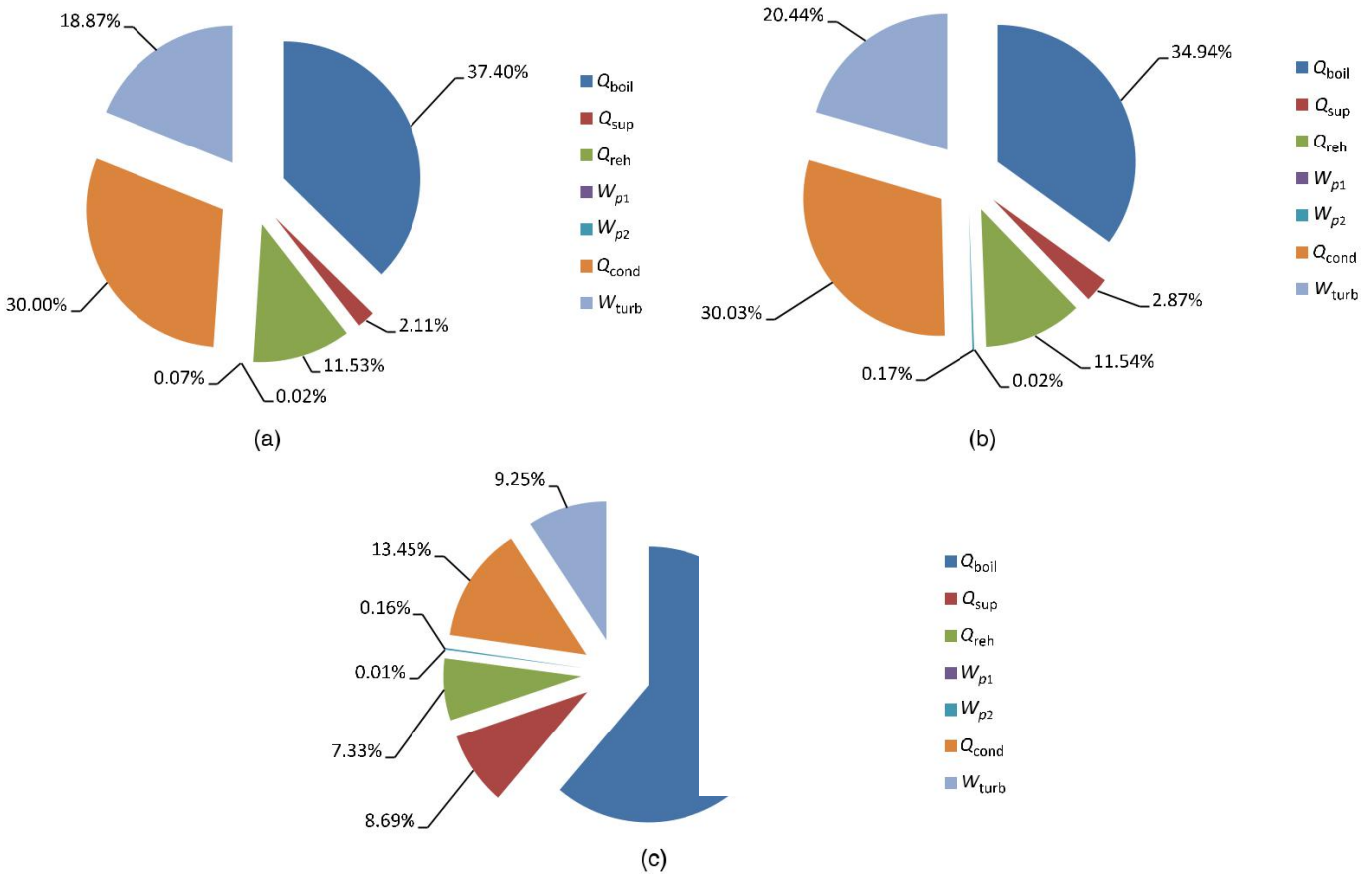

Fig. 3. Consolidated graphic TQR_{cyc} plot of the Rankine cycle for varying vaporizer pressure: (a) P_{vap} = 5 MPa; (b) P_{vap} = 10 MPa; (c) P_{vap} = 20 MPa for fixed values of the process parameters

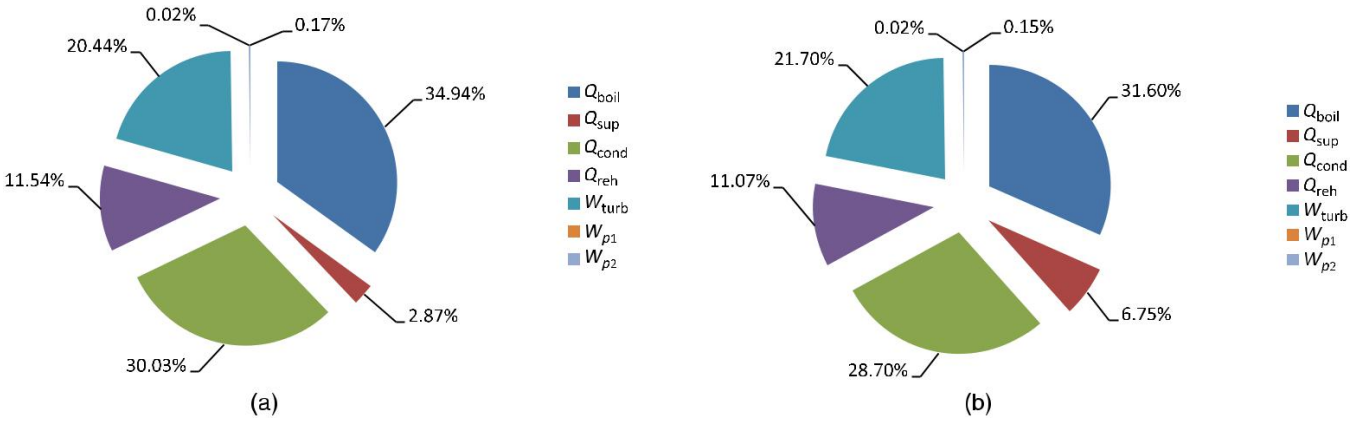

Fig. 4. Typical consolidated graphic TQR_{cyc} plot of the Rankine cycle for varying vaporizer temperature: (a) T_{vap} ¼ 400°C; (b) T_{vap} ¼ 500°C for fixed values of the process parameters

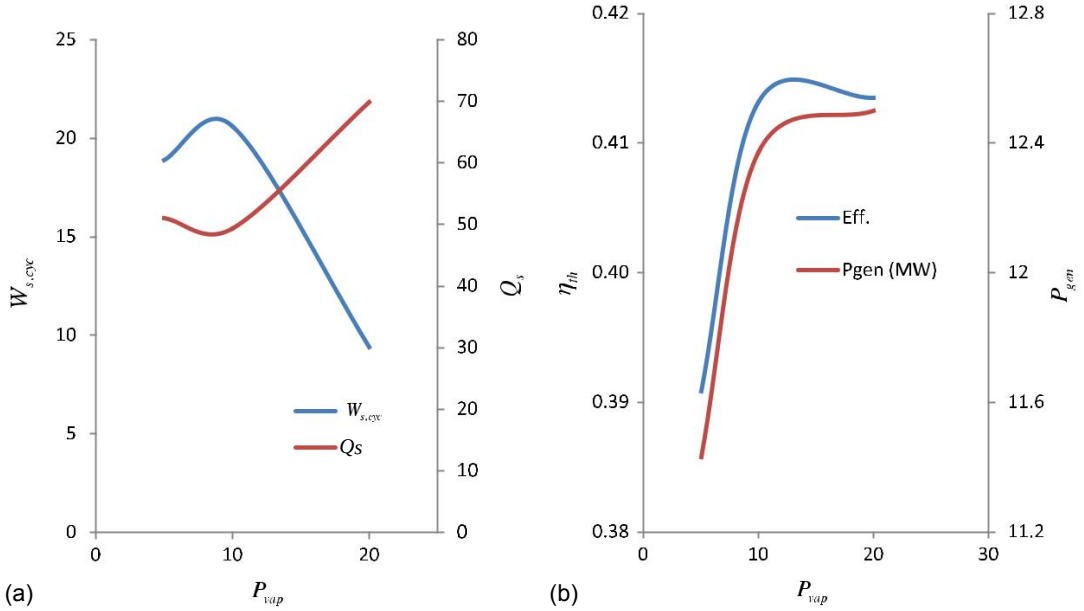

Fig. 5. (a) Plot of Q_s and $W_{s;cyc}$ with varying vaporizer pressure; (b) plot of P_{gen} and η_{th} with varying superheater (vaporizer) pressure

Downloaded

respect to the operating pressure, as such translating to potentially high cost of power generation. Thus, operating a thermal plant at peak efficiency does not necessarily entail the least cost of power production, and this can translate not just to high operational and maintenance costs but also increased tariff to the consumer and adverse environmental consequences. If the economics and sustainability of thermal operations are key considerations in the operations of a thermal plant, a judicious choice must be made. Beyond the optimal P_{vap} values, however, the difference in power output is marginal with potentially high operating expense.

Plots of Q_s, $W_{s;cyc}$, P_{gen}, and η_{th} in connection with vaporizer pressure, P_{vap} are given in Figs. 5 and 6, and show the influence of the vaporizer pressure on the heat and work quantities. Q_s is defined by Q_s ¼ Q_{sup} : þ $Q_{boil.}$ and $W_{s;cyc}$ given by $W_{s;cyc}$ ¼ W_{p1} þ W_{t1} .. ($Q_{cond:}$ is dissipated, therefore omitted not an energy expense/heat input quantity). The generated power is seen to increase with increasing vaporizer pressure, P_{vap} in the figure. The thermal efficiency is seen to increase with the generated power P_{gen} as vaporizer pressure increases, indicating that a high degree of superheat is favorable for improved efficiency.

Fig. 5(b) gives emphasis to the fact that the point of maximum thermal efficiency does not necessarily entail the point of optimal operating pressure. At P_{vap} values of 5 and 20 MPa, respectively, less power is generated per KJ of heat addition, although marginally, compared to that at P_{vap} ≈ 10 MPa.

The PQR ratio gives an indication of the fuel-to-power conversion ratios. High PQR values suggest increasing power output relative to heat (fuel) input. It is seen that at the point where the ratio is maximum, the generated power is relatively high. Consequently, operating commercial (conventional and alternative energy) plants at the optimum power generating capacity

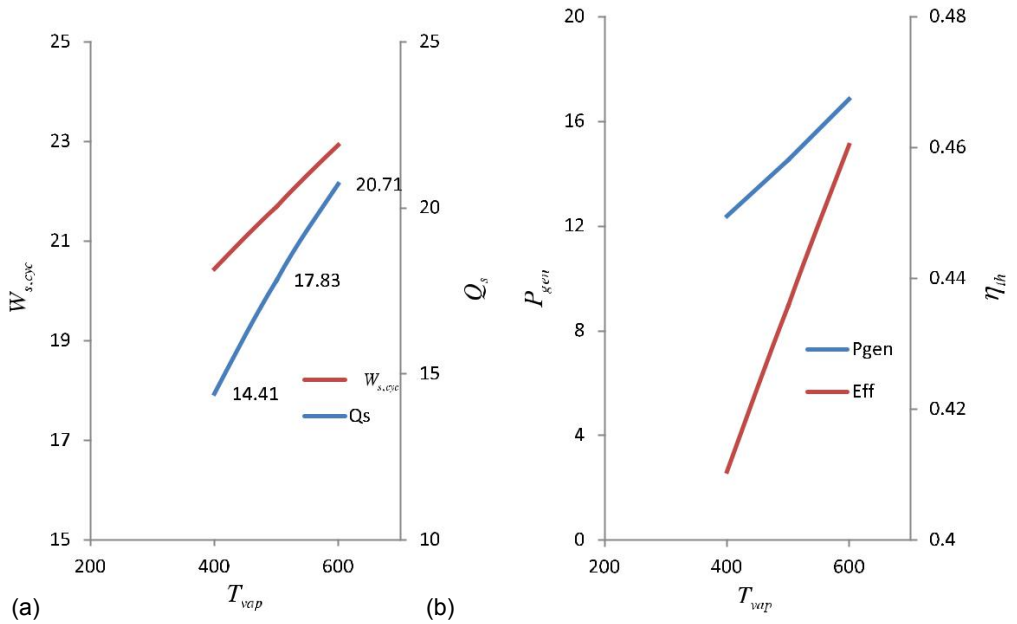

Fig. 6. (a) Plot of Q_s and $W_{s;cyc}$ with varying superheater (vaporizer) pressure; (b) plot of P_{gen} and η_{th} with varying superheater (vaporizer) pressure

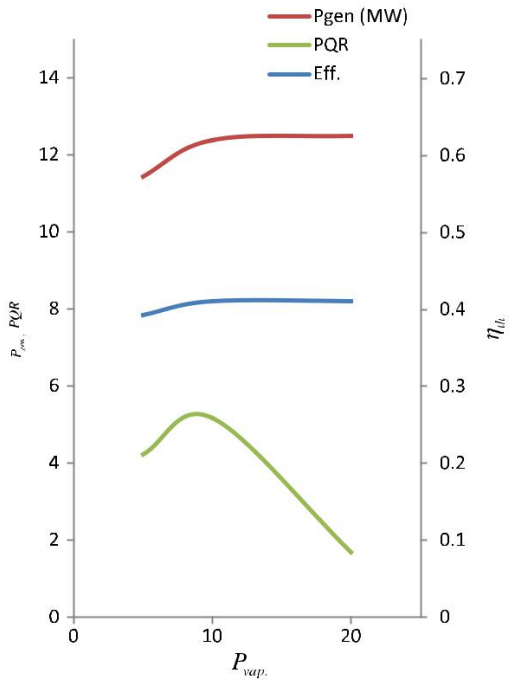

Fig. 7. Plot of P_{gen}, PQR and η_{th} with varying vaporizer pressure

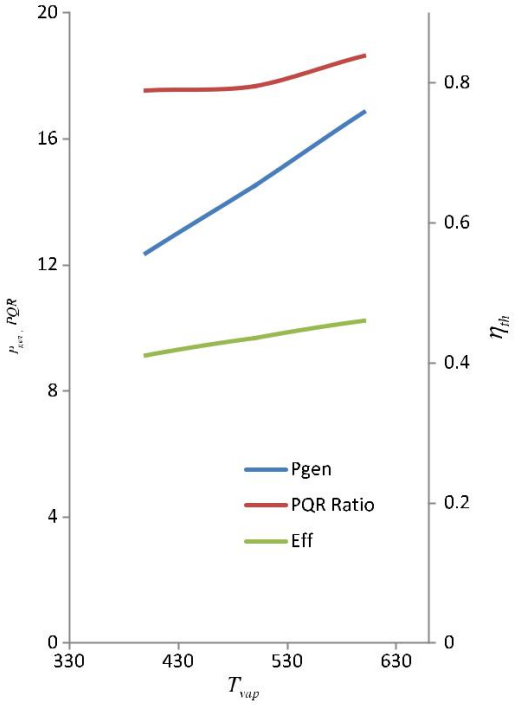

Fig. 8. Plot of P_{gen}, PQR and η_{th} with varying vaporizer temperature

rather than the peak operating capacity will potentially save operational costs.

In Fig. 6, the thermal efficiency is seen to increase with the gen-erated power P_{gen} and vaporizer temperature T_{vap}—an indication of the influence of the degree of superheat. In Figs. 7 and 8, it is seen that at the point where PQR is maximum, the generated power ap-proaches the maximum value. Importantly, in this case maximum PQR as in the foregoing, gives an indication of an energy-effective and cost-effective operation, when compared with thermal effi-ciency plots in the figures.

Conclusion

This study presented a method of thermodynamic optimization of power generating plants. The optimization methodology is em-ployed in identifying the technical and process parameters that are necessary to improving the thermodynamic performance of a power plant. Comparatively, the thermodynamic optimization mea-sures are approached by considering the objectives of operating the plant at the maximum thermodynamic and economic benefits by determining the input and output variables required to operate

the plant in a thermodynamically optimal state; this in turn affects the sustainability of the operations. The optimization of the funda-mental thermodynamic variables is critical to maintaining profitable, energy-efficient operations in a thermal plant. Temperature and pressure are the fundamental variables of any thermodynamic process, as such intricately linked to work output and energy expense (heat input) in the system. In this work, a thermodynamic study of a multi-stage CSP Rankine plant is undertaken. Simple but effective models are used to indicate graphically and otherwise the thermodynamic quantities in the plant, and evaluate the optimal and suboptimal power generating capacities vis-à-vis the fundamental variables. Results indicate that the PQR can be used to delineate the optimal values of the process variables as opposed to thermal efficiency-based plots; beyond the optimal value of the objective variable, the optimal power generation capacity of the plant is impacted. The methodology of obtaining the optimal value of the objective variable can also be approached by computerization.

Notation

The following symbols are used in this paper:

b; in = system boundary, in;
b; out = system boundary, out;
E = power (W);
h = enthalpy (KJ=kg);
m = mass fraction;
$\dot{m}$ = mass flow rate (kg=s);
P = pressure (Pa);
P_t = turbine (generated) power (W);
Q = heat (KJ=kg);
S_{gen} = entropy generation (KJ=kg K);
s = entropy (KJ=kg);
T = temperature (W);
W = work (KJ=kg);
0 = destroyed;
υ = specific volume (m^3=kg);
η = efficiency;
E_{system} = energy difference (KJ=kg); and
ke_s = potential energy difference (KJ=kg).

Subscripts

boil. = boiler;
cond. = condenser;
dest. = destroyed;
e = temperature (W);
i = intermediate;
in = in; out
= outlet;
p = pump;
reh. = reheater;
sink = pump;
source = pump;
sup. = superheater; and
t = turbine.

References

Ankur, G., and Khandwawala, A. I. (2013). "Thermodynamic analysis of 120 MW thermal power plant with combined effect of constant inlet pressure (124.61 bar) and different inlet temperature." Case Stud. Therm. Eng., 1(1), 17–25.

Badr, O., Probert, D. S., and O'Callaghan, P. W. (1985). "Selecting a working fluid for a Rankine-cycle engine." Appl. Energy, 21(1), 1–42.

Clarke, J. (2014). "Optimal design of geothermal power plants theses and dissertations." Graduate School, Virginia Commonwealth Univ., VCU Scholars Compass, Richmond, VA.

Ho, T., Samuel, M. S., and Ralph, G. (2012). "Comparison of the organic flash cycle (OFC) to other advanced vapor cycles for intermediate and high temperature waste heat reclamation and solar thermal energy." Energy, 42(1), 213–223.

Huijuan, C. D., Yogi, G., and Stefanakos, E. K. (2010). "A review of thermodynamic cycles and working fluids for the conversion of low-grade heat." Renewable Sustainable Energy Rev., 14(9), 3059–3067.

Kapooria, K. R., Kumar, S., and Kasana, K. S. (2008). "An analysis of a thermal power plant working on a Rankine cycle: A theoretical investigation." J. Energy South. Afr., 19(1), 77–84.

Li, M., Wang, J., He, W., Wang, B., Ma, S., and Dai, Y. (2013). "Experimental evaluation of the regenerative and basic organic Rankine cycles for low-grade heat source utilization." J. Energy Eng., 10.1061/(ASCE) EY.1943-7897.0000120, 190–197.

Mu, Y., Zhang, Y., Deng, N., and Nie, J. (2015). "Experimental study of a low-temperature power generation system in an organic Rankine cycle." J. Energy Eng., 10.1061/(ASCE)EY.1943-7897.0000181, 04014017.

Nouman, J. (2012). "Comparative studies and analyses of working fluids for organic Rankine cycles—ORC." M.Sc. thesis, KTH School of Industrial Engineering and Management Energy Technology, Stockholm, Sweden.

Roy, J. P., and Misra, A. (2012). "Parametric optimization and performance analysis of a regenerative organic Rankine cycle using R-123 for waste heat recovery." Energy, 39(1), 227–235.

Siemens AG. (2010). "Siemens steam turbines for CSP plants industrial steam turbines answers for energy." ⟨http://www.energy.siemens.com/mx/pool/hq/power-generation/steam-turbines/downloads/brochure-orc-organic-Rankine-cycle-technology_EN.pdf⟩.

Wanga, J., Yana, Z., Wanga, M., Maa, S., and Daia, Y. (2013). "Thermodynamic analysis and optimization of an (organic Rankine cycle) ORC using low grade heat source." Energy, 49(1), 356–365.

Yekoladio, P. J., Bello-Ochende, T., and Meyer, P. J. (2015). "Thermodynamic analysis and performance optimization of organic Rankine cycles for the conversion of low-to-moderate grade geothermal heat." Int. J. Energy Res., 39(9), 1256–1271.

Yunus, A. C., and Michael, A. B. (2006). Thermodynamics: An engineering approach, 5th Ed., McGraw-Hill, Boston, 551–584.